

Keywords: coordination polymer; lanthanide; 2-aminoterephthalic acid; oxalic acid; crystal structure.

CCDC reference: 1962371

Supporting information: this article has supporting information at journals.iucr.org/e

Organically pillared layer framework of [Eu(NH₂-BDC)(ox)(H₃O)]

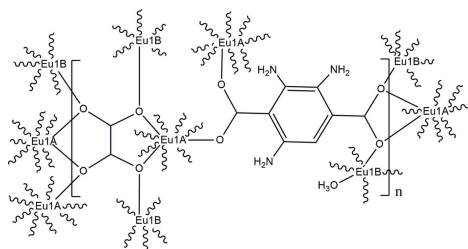
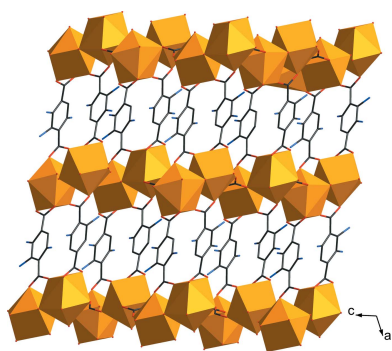
Supaphorn Thammakan,^a Kitt Panyarat^a and Apinpus Rujiwatra^{a,b,*}

^aDepartment of Chemistry, Faculty of Science, Chiang Mai University, Chiang Mai, 50200, Thailand, and ^bMaterials Science Research Center, Faculty of Science, Chiang Mai University, Chiang Mai 50200, Thailand. *Correspondence e-mail: apinpus.rujiwatra@cmu.ac.th

The non-porous three-dimensional structure of poly[(μ_5 -2-aminobenzene-1,4-dicarboxylato)(μ_6 -oxalato)(oxomium)europium(III)], [Eu(C₈H₅NO₄)(C₂O₄)(H₃O)]_n or [Eu^{III}(NH₂-BDC)(ox)(H₃O)]_n (NH₂-BDC²⁻ = 2-aminoterephthalate and ox²⁻ = oxalate) is constructed from two-dimensional layers of Eu^{III}-carboxylate-oxalate, which are connected by NH₂-BDC²⁻ pillars. The basic structural unit of the layer is an edge-sharing dimer of TPRS-{Eu^{III}O₉}, which is assembled through the ox²⁻ moiety. The intralayer void is partially occupied by TPR-{Eu^{III}O₆} motifs. Weak C—H···O and strong, classical intramolecular N—H···O and intermolecular O—H···O hydrogen-bonding interactions, as well as weak π - π stacking interactions, affix the organic pillars within the framework. The two-dimensional layer can be simplified to a uninodal 4-connected **sql/Shubnikov tetragonal plane** net with point symbol {4⁴.6²}.

1. Chemical context

Lanthanide coordination polymers (LnCPs) have emerged as authentic multifunctional materials finding potential in various applications, *e.g.* magnetism, optics, luminescence and in heterogeneous catalysis (Roy *et al.*, 2014). In the crystal engineering of LnCPs, the judicious choice of organic ligands is critical. Among the widely employed dicarboxylates, 1,4-benzenedicarboxylic acid (H₂BDC) tends to provide three-dimensional frameworks with permanent porosity. To enhance interactions with guest species, additional functional groups can be introduced onto the phenyl ring of BDC²⁻, *e.g.* 2-amino-1,4-benzenedicarboxylic acid (NH₂-H₂BDC) in NH₂-MIL-53(AI) enhanced the carbon dioxide capture capacity (Stavitski *et al.*, 2011; Flaig *et al.*, 2017; Wang *et al.*, 2012). The smallest dicarboxylic acid, *i.e.* oxalic acid (H₂ox), on the other hand, may not facilitate the porous framework (Zhang *et al.*, 2016; Xiahou *et al.*, 2013) and its presence as a secondary ligand in the fabrication may lead to diversity in the framework structures.



Herein, NH₂-H₂BDC and H₂ox were employed as mixed linkers in the synthesis of a new three-dimensional framework of europium, *i.e.* [Eu(NH₂-BDC)(ox)(H₃O)] (**I**). The crystal

structure of **I**, which exhibits site disorder at both the Eu^{III} ion and the amino group, is reported. Weak intermolecular interactions and the framework topology are also described.

2. Structural commentary

$[\text{Eu}(\text{NH}_2\text{-BDC})(\text{ox})(\text{H}_3\text{O})]$ crystallizes in the monoclinic space group $P2_1/c$. Its asymmetric unit comprises one Eu^{III} ion, which is disordered over two crystallographic sites with an occupying ratio of 0.86 (Eu1A): 0.14 (Eu1B) and whole molecules of $\text{NH}_2\text{-BDC}^{2-}$, ox^{2-} and H_3O^+ (Fig. 1). Eu1A is ninefold coordinated to nine O atoms from one chelating $\text{NH}_2\text{-BDC}^{2-}$, two monodentate $\text{NH}_2\text{-BDC}^{2-}$, two chelating ox^{2-} and one monodentate ox^{2-} groups, all of which delineate into a distorted tricapped trigonal-prismatic geometry, *i.e.* $\text{TPRS}\{-\text{Eu}^{\text{III}}\text{O}_9\}$. Eu1B, on the other hand, adopts a sixfold

coordination of trigonal anti-prismatic geometry, *i.e.* $\text{TPR}\{-\text{Eu}^{\text{III}}\text{O}_6\}$, which is completed by six O atoms from two monodentate $\text{NH}_2\text{-BDC}^{2-}$, three monodentate ox^{2-} and one H_3O^+ moieties. Noticeably, the three monodentate ox^{2-} moieties form one trigonal face whereas the two monodentate $\text{NH}_2\text{-BDC}^{2-}$ and the ligated H_3O^+ moieties outline the other. The $\text{Eu}^{\text{III}}\text{-O}$ bond distances ranging between 2.375 (2) and 2.562 (2) Å, are consistent with the values observed for other Eu^{III} coordination frameworks, *e.g.* $[(\text{CH}_3)_2\text{NH}_2]_2\text{-}[\text{Eu}_6(\mu_3\text{-OH})_8(\text{BDC-NH}_2)_6(\text{H}_2\text{O})_6]$ (Yi *et al.*, 2016) and $[\text{Eu}_2(\text{ATPA})_3(\text{DEF})_2]_n$ where ATPA^{2-} = 2-aminoterephthalate and DEF = diethylformamide (Kariem *et al.*, 2016). In addition to the disorder at the Eu^{III} positions, there is an additional disorder at the amino group of $\text{NH}_2\text{-BDC}^{2-}$, which distributes over three crystallographic sites with site occupancies of 0.26 (N1), 0.44 (N2) and 0.31 (N3), respectively.

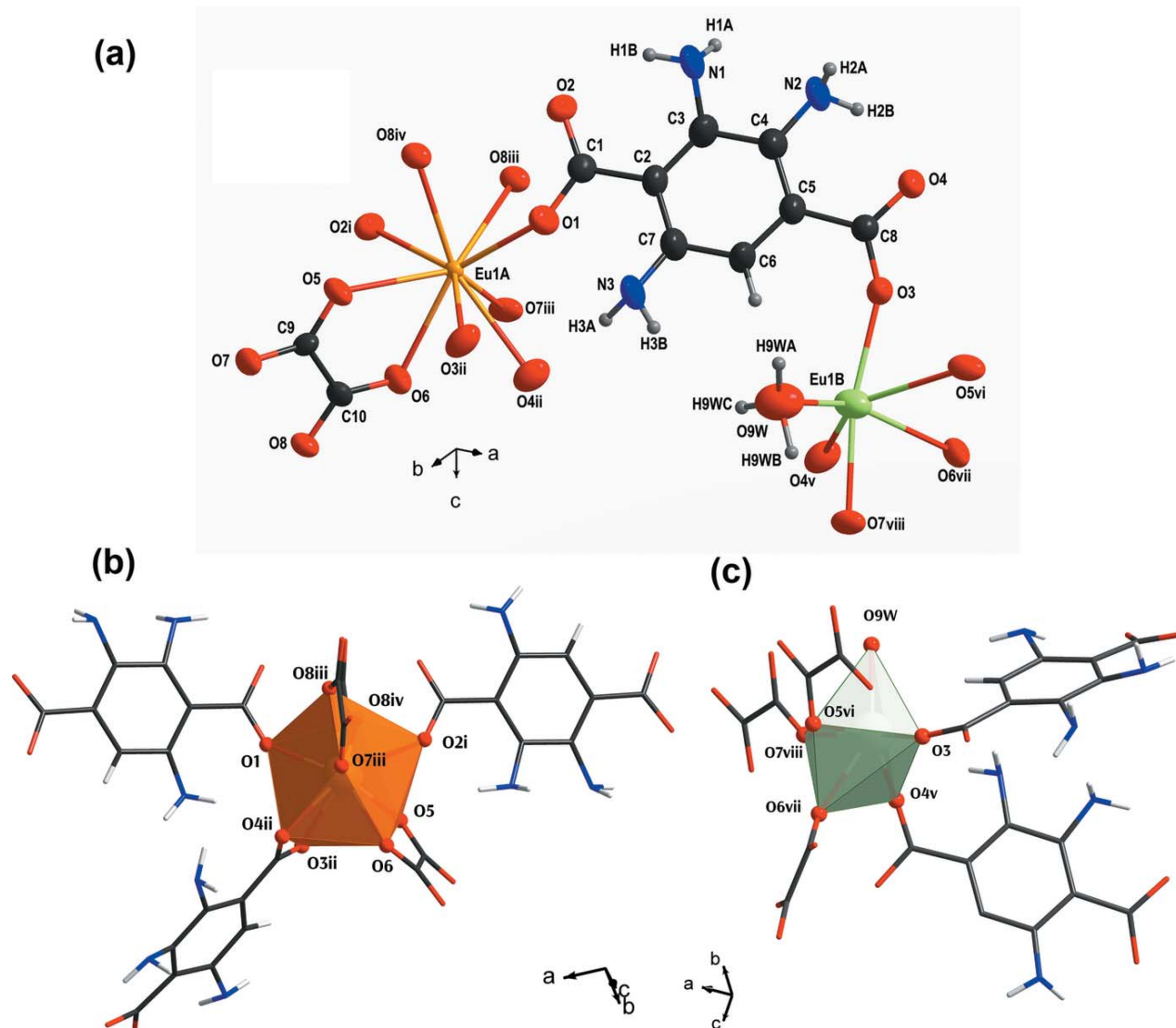


Figure 1
Views of (a) an extended asymmetric unit of **I** drawn using 60% probability ellipsoids and the coordination environments about (b) Eu1A and (c) Eu1B. [Symmetry codes: (i) $-x, 1 - y, -z$; (ii) $1 - x, \frac{1}{2} + y, \frac{1}{2} - z$; (iii) $-x, -\frac{1}{2} + y, \frac{1}{2} - z$; (iv) $x, \frac{3}{2} - y, -\frac{1}{2} + z$; (v) $x, \frac{1}{2} - y, \frac{1}{2} + z$; (vi) $1 - x, -\frac{1}{2} + y, \frac{1}{2} - z$; (vii) $1 - x, 1 - y, 1 - z$; (viii) $1 - x, \frac{3}{2} - y, \frac{1}{2} + z$.]

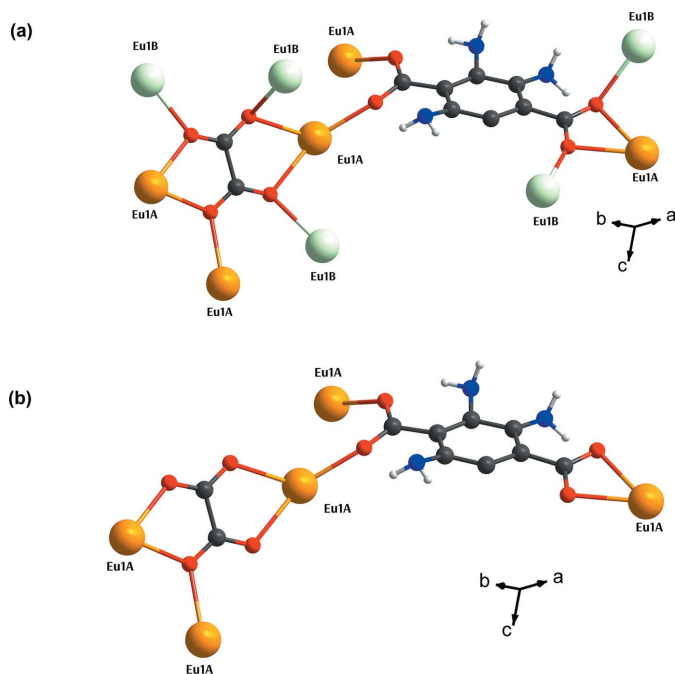


Figure 2
 Depictions of coordination modes adopted by $\text{NH}_2\text{-BDC}^{2-}$ and ox^{2-} ; (a) with (b) without Eu1B .

As a result of the disorder of the Eu^{III} ion, the modes of coordinations for both $\text{NH}_2\text{-BDC}^{2-}$ and ox^{2-} are diverse. If all of the possible sites of Eu^{III} are concurrently included, the $\mu_5\text{-}\eta^1\text{:}\eta^1\text{:}\eta^2\text{:}\eta^2$ mode can be assigned to $\text{NH}_2\text{-BDC}^{2-}$ as it connects three Eu1A and two Eu1B moieties together (Fig. 2). In a similar fashion, three Eu1A and three Eu1B moieties may be simultaneously linked by ox^{2-} using the $\mu_6\text{-}\eta^2\text{:}\eta^2\text{:}\eta^2\text{:}\eta^2$ mode for coordination. It is worth noting that the

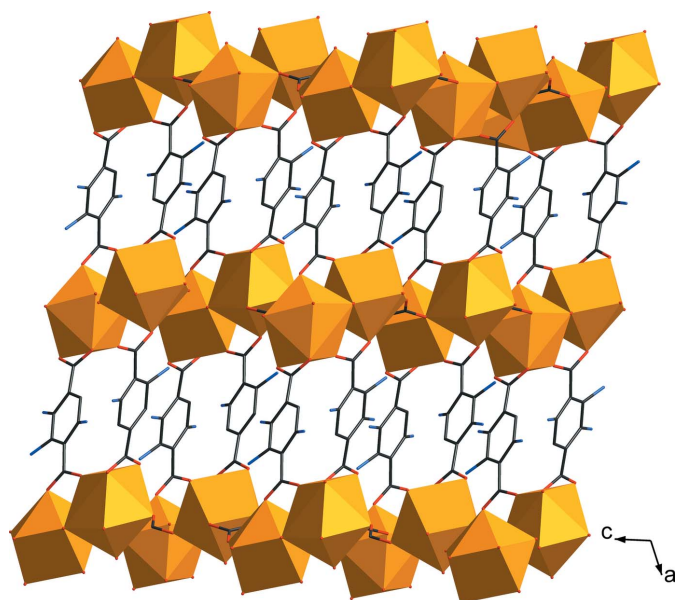


Figure 3
 The three-dimensional framework structure of **I**.

Table 1
 Hydrogen-bond geometry (\AA , $^\circ$).

$D\text{-H}\cdots A$	$D\text{-H}$	$\text{H}\cdots A$	$D\cdots A$	$D\text{-H}\cdots A$
$\text{O9W-H9WA}\cdots\text{O2}^{\text{i}}$	1.11 (5)	1.81 (5)	2.904 (4)	171 (5)
$\text{O9W-H9WB}\cdots\text{O5}^{\text{ii}}$	1.10 (5)	1.87 (5)	2.943 (4)	163 (4)
$\text{C6-H6}\cdots\text{O3}$	0.93	2.47	2.781 (6)	100
$\text{N1-H1B}\cdots\text{O2}$	0.86	2.03	2.736 (16)	139

Symmetry codes: (i) $-x+1, -y+1, -z$; (ii) $x+1, -y+\frac{3}{2}, z+\frac{1}{2}$.

$\mu_5\text{-}\eta^1\text{:}\eta^1\text{:}\eta^2\text{:}\eta^2$ mode of $\text{NH}_2\text{-BDC}^{2-}$ and the $\mu_6\text{-}\eta^2\text{:}\eta^2\text{:}\eta^2\text{:}\eta^2$ mode of ox^{2-} are unprecedented. If only the dominating Eu1A is regarded, the adopted coordination modes would be $\mu_3\text{-}\eta^1\text{:}\eta^1\text{:}\eta^1$ and $\mu_3\text{-}\eta^1\text{:}\eta^1\text{:}\eta^2$ for $\text{NH}_2\text{-BDC}^{2-}$ and ox^{2-} , respectively. Likewise, there are only sixteen structures containing ox^{2-} with a $\mu_3\text{-}\eta^1\text{:}\eta^1\text{:}\eta^2$ mode and only two LnCPs comprising $\text{NH}_2\text{-BDC}^{2-}$ with a $\mu_3\text{-}\eta^1\text{:}\eta^1\text{:}\eta^1$ mode, i.e. $[\text{Yb}_2(\text{OH})(\text{atpt})_{2.5}(\text{phen})_2]_n \cdot 1.75n\text{H}_2\text{O}$ where $\text{atpt}^{2-} = 2\text{-aminoterephthalate}$ and $\text{phen} = 1,10\text{-phenanthroline}$ (Liu *et al.*, 2004), and $\{[\text{Ho}_2(\mu_3\text{-ATA})_2(\mu_4\text{-ATA})(\text{H}_2\text{O})_4] \cdot 2\text{DMF} \cdot 0.5\text{H}_2\text{O}\}_n$ where $\text{ATA}^{2-} = 2\text{-aminoterephthalate}$ (Almási *et al.*, 2014).

3. Supramolecular features

The structure of **I** features a three-dimensional framework, which can be regarded as being built up of two-dimensional layers of Eu^{III} -carboxylate-oxalate connected by the $\text{NH}_2\text{-BDC}^{2-}$ organic pillars (Fig. 3). The basic building motif of the layer is the edge-sharing dimer of $\text{TPRS}\text{-}\{\text{Eu}^{\text{III}}\text{O}_9\}$ (Fig. 4), which is fused together through two O8 atoms from two ox^{2-} groups and two O1-C1-O2 bridges of two $\text{NH}_2\text{-BDC}^{2-}$.

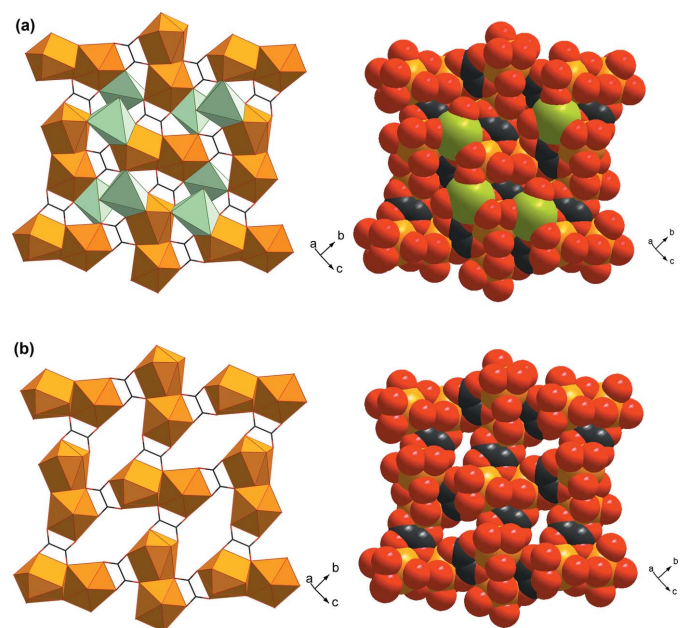


Figure 4
 Polyhedral and space-filling representations of the Eu^{III} -oxalate-carboxylate layers (a) with $\text{TPR}\text{-}\{\text{Eu}^{\text{III}}\text{O}_6\}$ motifs and (b) without $\text{TPR}\text{-}\{\text{Eu}^{\text{III}}\text{O}_6\}$ motif.

Each $\{\text{Eu}_2^{\text{III}}\text{O}_{16}\}$ dimer of **Eu1A** is tied to the other four equivalent dimers through four ox^{2-} linkers in the bc plane. The as-described arrangement of these $\{\text{Eu}_2^{\text{III}}\text{O}_{16}\}$ dimers creates voids characterized as the twelve-membered rings, in which the partially occupied $\text{TPR}\{-\text{Eu}^{\text{III}}\text{O}_6\}$ motifs of **Eu1B** are situated. Each of the $\text{TPR}\{-\text{Eu}^{\text{III}}\text{O}_6\}$ motifs are affixed within the layer through four O atoms from four surrounding ox^{2-} groups and an O4 atom from $\text{NH}_2\text{-BDC}^{2-}$. These layers are further connected by the $\text{NH}_2\text{-BDC}^{2-}$ organic pillars along the a -axis direction providing the non-porous three-dimensional framework. The roles of ox^{2-} and $\text{NH}_2\text{-BDC}^{2-}$ in the framework of **I** are, therefore, to create the layer framework and to tether the layers, respectively.

The $\text{NH}_2\text{-BDC}^{2-}$ pillar is apparently organized through intramolecular hydrogen-bonding interactions from both strong $\text{N-H}\cdots\text{O}$ and weak $\text{C-H}\cdots\text{O}$ interactions (Table 1), and through the face-to-face antiparallel displaced $\pi\text{-}\pi$ interactions (Banerjee *et al.*, 2019) established between the phenyl rings of two adjacent $\text{NH}_2\text{-BDC}^{2-}$ pillars (Fig. 5). In addition to the intramolecular hydrogen-bonding interactions, two H atoms from the H_3O^+ molecule are also involved in providing additional strong $\text{O-H}\cdots\text{O}$ intermolecular hydrogen-bonding interactions.

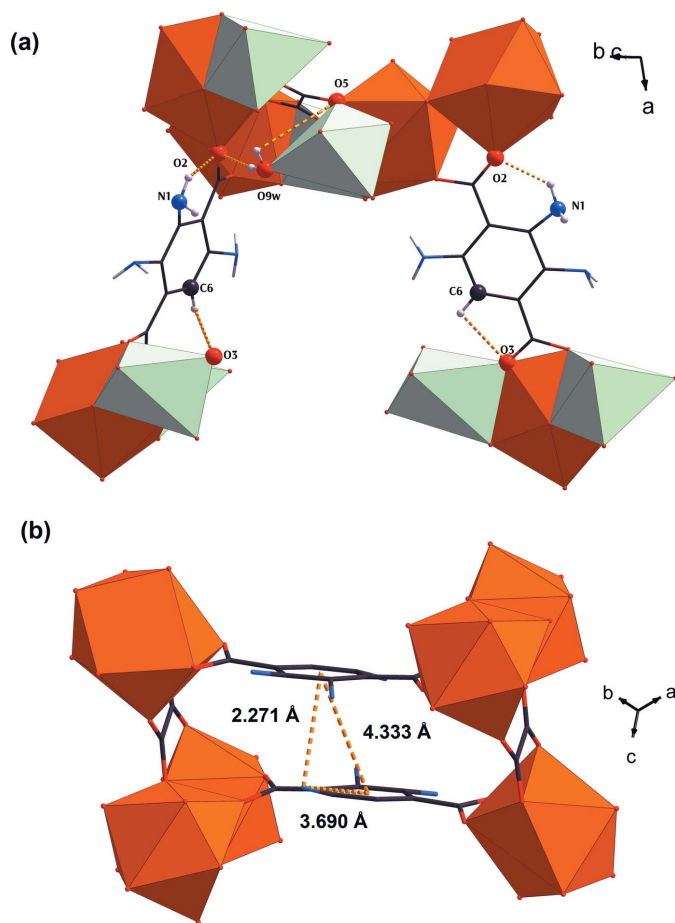


Figure 5
Views of (a) the hydrogen-bonding interactions and (b) the $\pi\text{-}\pi$ interactions.

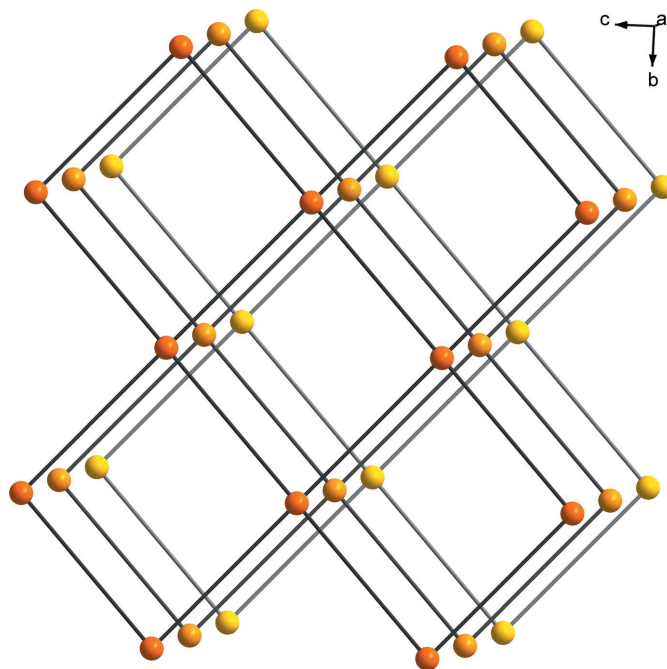


Figure 6
The simplified two- and three-dimensional topologies of **I**.

4. Topology

The topology of the two-dimensional layer of **I** was analysed using *TOPOS* software (Blatov, 2004). If only the dominating motif, *i.e.* the edge-sharing dimer of **Eu1A**, is taken as a node, which is connected to the other equivalent dimer *via* the ox^{2-} linker, the two-dimensional layer of **Eu1** can be simplified to a uninodal 4-connected **sql/Shubnikov tetragonal plane** net with a point symbol $\{4^4.6^2\}$ (Blatov *et al.*, 2014) (Fig. 6). The inclusion of the partially occupied $\text{TPR}\{-\text{Eu}^{\text{III}}\text{O}_6\}$ motifs results in unknown topology. This is also the case for the three-dimensional framework with or without the $\text{TPR}\{-\text{Eu}^{\text{III}}\text{O}_6\}$ motifs.

5. Photoluminescent property

A room temperature photoluminescent spectrum of **I** was collected (Jasco FB-8500 spectrofluorometer, $\lambda_{\text{excitation}} = 337$ nm). It exhibits none of the characteristic $f\text{-}f$ emission of Eu^{III} . Even the broad emission characteristic of the ligand-centered $\pi\text{-}\pi$ emission was not observed. This may be attributed to a proton-induced fluorescence-quenching mechanism facilitated by the presence of H_3O^+ in close proximity to the phenyl ring of $\text{NH}_2\text{-BDC}^{2-}$ (Tobita & Shizuka, 1980; Shizuka & Tobita, 1982). The quenching consequently hinders the sensitization, which is important according to the antenna model (Einkauf *et al.*, 2017).

6. Database survey

Based on a survey of the Cambridge Structural Database (version 5.40, Nov 2018 with the update of May 2019; Groom *et al.*, 2016), no LnCP containing both $\text{NH}_2\text{-BDC}^{2-}$ and ox^{2-}

Table 2
Experimental details.

Crystal data	
Chemical formula	[Eu(C ₈ H ₅ NO ₄)(C ₂ O ₄)(H ₃ O)]
<i>M_r</i>	436.32
Crystal system, space group	Monoclinic, <i>P</i> ₂ /c
Temperature (K)	293
<i>a</i> , <i>b</i> , <i>c</i> (Å)	11.8348 (3), 11.3208 (3), 10.6531 (3)
β (°)	110.275 (3)
<i>V</i> (Å ³)	1338.86 (7)
<i>Z</i>	4
Radiation type	Mo <i>K</i> α
μ (mm ⁻¹)	4.73
Crystal size (mm)	0.2 × 0.05 × 0.05
Data collection	
Diffraction	Rigaku OD SuperNova, single source at offset/far, HyPix3000
Absorption correction	Multi-scan (<i>CrysAlis PRO</i> ; Rigaku OD, 2018)
<i>T</i> _{min} , <i>T</i> _{max}	0.753, 0.789
No. of measured, independent and observed [<i>I</i> > 2 σ (<i>I</i>)] reflections	15479, 2882, 2458
<i>R</i> _{int}	0.050
(<i>sin</i> θ / λ) _{max} (Å ⁻¹)	0.647
Refinement	
<i>R</i> [<i>F</i> ² > 2 σ (<i>F</i> ²)], <i>wR</i> (<i>F</i> ²), <i>S</i>	0.028, 0.067, 1.09
No. of reflections	2882
No. of parameters	222
No. of restraints	4
H-atom treatment	H atoms treated by a mixture of independent and constrained refinement
$\Delta\rho_{\max}$, $\Delta\rho_{\min}$ (e Å ⁻³)	0.61, -0.54

Computer programs: *CrysAlis PRO* (Rigaku OD, 2018), *SHELXT* (Sheldrick, 2015b), *SHELXL* (Sheldrick, 2015a) and *OLEX2* (Dolomanov *et al.*, 2009).

has previously been reported. However, there are three closely relevant structures which have similar unit-cell parameters, *i.e.* *catena*-[(μ -tetracyanoborate)tetraaquabis(nitrate)lanthanum] (Zotnick *et al.*, 2017), *catena*-[hemikis(piperazinedium)(μ -benzene-1,2,4,5-tetracarboxylato)diaquaprasedymium(III)] (Liang *et al.*, 2017) and η^5 -indenyl)dichlorotris(tetrahydrofuran-*O*)gadolinium tetrahydrofuran solvate (Fuxing *et al.*, 1992).

7. Synthesis and crystallization

To synthesize **I**, 2-aminoterephthalic acid (0.2 mmol, 0.0332 g), oxalic acid (0.2 mmol, 0.0180 g) and 1,4-diazabicyclo[2.2.2]-octane (0.4 mmol, 0.0448 g) were dissolved in 8.0 mL of DMF/H₂O (1 m:7 mL) to prepare solution **A**. Separately, solution **B** was prepared by dissolving Eu₂O₃ (0.1 mmol, 0.0180 g) in 1.0 mL of concentrated HNO₃ aqueous solution, which was then adjusted to pH 7 using a 10 M NaOH aqueous solution. Solution **B** was then gradually introduced into solution **A**, and the mixture was then transferred to a 22 mL Teflon-lined stainless-steel autoclave. The reaction was carried out under an autogenous pressure generated at 393 K for 7 days. Yellow crystals of **I** were then recovered by filtration. FT-IR of **I** (KBr; cm⁻¹): 3361, 2987, 1617, 1313, 1053, 798.

8. Refinement

Crystal data, data collection and structure refinement details are summarized in Table 2. The Eu^{III} ion was refined as being disordered over two crystallographic sites resulting in refined occupancies of 0.855 (Eu1A) and 0.145 (Eu1B). The disorder of the amino group over three crystallographic sites could be clearly seen in the electron-density map and was refined using the SUMP command providing occupancies of 0.259 (N1), 0.440 (N2) and 0.305 (N3). EADP constraints were necessary to make the anisotropic refinements of the disordered N atoms stable. The three H atoms on the ligated H₃O⁺ (O9W) were evident in the electron-density map and therefore assigned as such. The SADI restraint was nonetheless applied on the refinements of the three O–H bonds. H atoms could be positioned from the electron-density maps and were refined as riding with *U*_{iso}(H) = 1.2*U*_{eq}(C, N) or 1.5*U*_{eq}(O). Bond restraints on N–H and O–H were applied in the refinements.

Funding information

Funding for this research was co-provided by: Chiang Mai University and Thailand Research Fund (grant No. RSA6280003 to Apinpus Rujiwattra); Science Achievement Scholarship of Thailand (to Supaphorn Thammakan).

References

- Almáši, M., Zelená, V., Galdun, L. & Kuchár, J. (2014). *Inorg. Chem. Commun.* **39**, 39–42.
- Banerjee, A., Saha, A. & Saha, B. K. (2019). *Cryst. Growth Des.* **19**, 2245–2252.
- Blatov, V. A. (2004). *TOPOS*. Samara State University, Russia.
- Blatov, V. A., Shevchenko, A. P. & Proserpio, D. M. (2014). *Cryst. Growth Des.* **14**, 3576–3586.
- Dolomanov, O. V., Bourhis, L. J., Gildea, R. J., Howard, J. A. K. & Puschmann, H. (2009). *J. Appl. Cryst.* **42**, 339–341.
- Einkauf, J. D., Clark, J. M., Paulive, A., Tanner, G. P. & de Lill, D. T. (2017). *Inorg. Chem.* **56**, 5544–5552.
- Flaig, R. W., Popp, T. M. O., Fracaroli, A. M., Kapustin, E. A., Kalmutzki, M. J., Altamimi, R. M., Fathieh, F., Reimer, J. A. & Yaghi, O. M. (2017). *J. Am. Chem. Soc.* **139**, 12125–12128.
- Fuxing, G., Gecheng, W., Zhongsheng, J. & Wenqi, C. (1992). *J. Organomet. Chem.* **438**, 289–295.
- Groom, C. R., Bruno, I. J., Lightfoot, M. P. & Ward, S. C. (2016). *Acta Cryst.* **B72**, 171–179.
- Kariem, M., Yawer, M., Sharma, S. & Sheikh, H. N. (2016). *Chemistry Select*, **1**, 4489–4501.
- Liang, X.-Q. & Fan, Z.-L. (2017). *Chinese J. Struct. Chem.* **36**, 977–984.
- Liu, C.-B., Sun, C.-Y., Jin, L.-P. & Lu, S.-Z. (2004). *New J. Chem.* **28**, 1019–1026.
- Rigaku OD (2018). *CrysAlis PRO*. Rigaku Cooperation, Oxford, England.
- Roy, S., Charkraborty, A. & Maji, T.-K. (2014). *Chem. Rev.* **273–274**, 139–164.
- Sheldrick, G. M. (2015a). *Acta Cryst.* **A71**, 3–8.
- Sheldrick, G. M. (2015b). *Acta Cryst.* **C71**, 3–8.
- Shizuka, H. & Tobita, S. (1982). *J. Am. Chem. Soc.* **104**, 6919–6927.
- Stavitski, E., Pidko, E. A., Couck, S., Remy, T., Hensen, E. J. M., Weckhuysen, B. M., Denayer, J., Gascon, J. & Kapteijn, F. (2011). *Langmuir*, **27**, 3970–3976.
- Tobita, S. & Shizuka, H. (1980). *Chem. Phys. Lett.* **75**, 140–144.
- Wang, F., Tan, Y. X., Yang, H., Kang, Y. & Zhang, J. (2012). *Chem. Commun.* **48**, 4842–4844.

- Xiahou, Z.-J., Wang, Y.-L., Liu, Q.-Y., Li, L. & Zhou, L.-J. (2013). *J. Coord. Chem.* **66**, 2910–2918.
- Yi, P., Huang, H., Peng, Y., Liu, D. & Zhong, C. (2016). *RSC Adv.* **6**, 111934–111941.
- Zhang, X. T., Fan, L.-M., Fan, W.-L., Li, B., Liu, G. Z., Liu, X.-Z. & Zhao, X. (2016). *Cryst. Growth & Des.* **16**, 3993–4004.
- Zottnick, S. H., Finze, M. & Müller-Buschbaum, K. (2017). *Chem. Commun.* **53**, 5193–5195.

supporting information

Acta Cryst. (2019). E75, 1833-1838 [https://doi.org/10.1107/S2056989019014713]

Organically pillared layer framework of [Eu(NH₂-BDC)(ox)(H₃O)]

Supaphorn Thammakan, Kitt Panyarat and Apinpus Rujiwatra

Computing details

Data collection: *CrysAlis PRO* (Rigaku OD, 2018); cell refinement: *CrysAlis PRO* (Rigaku OD, 2018); data reduction: *CrysAlis PRO* (Rigaku OD, 2018); program(s) used to solve structure: SHELXT (Sheldrick, 2015b); program(s) used to refine structure: SHELXL (Sheldrick, 2015a); molecular graphics: OLEX2 (Dolomanov *et al.*, 2009); software used to prepare material for publication: OLEX2 (Dolomanov *et al.*, 2009).

Poly[(μ₆-oxalato)(oxomium)(μ₅-2-aminobenzene-1,4-dicarboxylato)europium(III)]

Crystal data

[Eu(C₈H₅NO₄)(C₂O₄)(H₃O)]

M_r = 436.32

Monoclinic, *P2₁/c*

a = 11.8348 (3) Å

b = 11.3208 (3) Å

c = 10.6531 (3) Å

β = 110.275 (3)°

V = 1338.86 (7) Å³

Z = 4

F(000) = 832

D_x = 2.165 Mg m⁻³

Mo *Kα* radiation, λ = 0.71073 Å

Cell parameters from 9488 reflections

θ = 1.8–27.3°

μ = 4.73 mm⁻¹

T = 293 K

Block, clear light yellow

0.2 × 0.05 × 0.05 mm

Data collection

Rigaku OD SuperNova, single source at
offset/far, HyPix3000
diffractometer

Radiation source: micro-focus sealed X-ray tube

ω scans

Absorption correction: multi-scan

(*CrysAlis PRO*; Rigaku OD, 2018)

T_{min} = 0.753, *T_{max}* = 0.789

15479 measured reflections

2882 independent reflections

2458 reflections with *I* > 2σ(*I*)

R_{int} = 0.050

θ_{max} = 27.4°, θ_{min} = 1.8°

h = -14→15

k = -11→14

l = -13→13

Refinement

Refinement on *F*²

Least-squares matrix: full

R[*F*² > 2σ(*F*²)] = 0.028

wR(*F*²) = 0.067

S = 1.09

2882 reflections

222 parameters

4 restraints

Hydrogen site location: mixed

H atoms treated by a mixture of independent
and constrained refinement

w = 1/[σ²(*F_o*²) + (0.0305*P*)² + 0.0276*P*]

where *P* = (*F_o*² + 2*F_c*²)/3

(Δ/σ)_{max} = 0.001

Δρ_{max} = 0.61 e Å⁻³

Δρ_{min} = -0.54 e Å⁻³

Special details

Geometry. All esds (except the esd in the dihedral angle between two l.s. planes) are estimated using the full covariance matrix. The cell esds are taken into account individually in the estimation of esds in distances, angles and torsion angles; correlations between esds in cell parameters are only used when they are defined by crystal symmetry. An approximate (isotropic) treatment of cell esds is used for estimating esds involving l.s. planes.

Fractional atomic coordinates and isotropic or equivalent isotropic displacement parameters (\AA^2)

	<i>x</i>	<i>y</i>	<i>z</i>	$U_{\text{iso}}^*/U_{\text{eq}}$	Occ. (<1)
Eu1A	0.07429 (2)	0.61284 (2)	0.15674 (2)	0.01311 (9)	0.8558 (8)
O6	0.0486 (2)	0.7311 (2)	0.3456 (2)	0.0298 (6)	
O8	-0.0221 (2)	0.89620 (19)	0.4069 (3)	0.0248 (6)	
O5	-0.0175 (2)	0.8135 (2)	0.0928 (2)	0.0314 (6)	
O2	0.1449 (2)	0.4078 (2)	-0.1090 (3)	0.0315 (7)	
O7	-0.0772 (2)	0.9814 (2)	0.1603 (2)	0.0298 (6)	
O4	0.7236 (2)	0.1331 (2)	0.1432 (3)	0.0356 (7)	
O1	0.2130 (2)	0.5301 (3)	0.0649 (3)	0.0385 (7)	
O3	0.7668 (2)	0.2640 (2)	0.3050 (3)	0.0366 (7)	
C10	0.0008 (3)	0.8307 (3)	0.3236 (4)	0.0212 (8)	
C1	0.2274 (3)	0.4463 (4)	-0.0068 (4)	0.0278 (9)	
C9	-0.0344 (3)	0.8795 (3)	0.1784 (4)	0.0229 (9)	
C8	0.6941 (3)	0.2224 (4)	0.1960 (4)	0.0290 (9)	
C2	0.3499 (3)	0.3911 (3)	0.0360 (4)	0.0319 (10)	
C5	0.5750 (3)	0.2802 (4)	0.1344 (4)	0.0353 (10)	
C6	0.5557 (4)	0.3900 (4)	0.1808 (5)	0.0502 (14)	
H6	0.619345	0.426877	0.246414	0.060*	
C3	0.3677 (4)	0.2839 (4)	-0.0150 (5)	0.0513 (13)	
C7	0.4454 (4)	0.4470 (4)	0.1332 (5)	0.0480 (12)	
C4	0.4805 (4)	0.2271 (4)	0.0321 (5)	0.0528 (13)	
N2	0.4834 (8)	0.1125 (8)	-0.0128 (12)	0.066 (3)	0.439 (6)
H2A	0.512716	0.113790	-0.078500	0.080*	0.439 (6)
H2B	0.531521	0.063870	0.047841	0.080*	0.439 (6)
N3	0.4511 (10)	0.5604 (13)	0.1717 (14)	0.066 (3)	0.312 (6)
H3A	0.407927	0.583997	0.230300	0.080*	0.312 (6)
H3B	0.527520	0.590092	0.221251	0.080*	0.312 (6)
N1	0.2993 (12)	0.2381 (15)	-0.1365 (15)	0.066 (3)	0.261 (6)
H1A	0.286630	0.164575	-0.125872	0.080*	0.261 (6)
H1B	0.231669	0.274954	-0.165662	0.080*	0.261 (6)
Eu1B	0.82330 (16)	0.39654 (13)	0.47691 (17)	0.0427 (7)	0.1442 (8)
O9W	0.8080 (3)	0.5707 (3)	0.3580 (3)	0.0593 (9)	
H9WA	0.816 (5)	0.581 (4)	0.258 (4)	0.089*	
H9WB	0.881 (4)	0.620 (4)	0.433 (5)	0.089*	
H9WC	0.725 (4)	0.578 (6)	0.383 (7)	0.15 (3)*	

Atomic displacement parameters (\AA^2)

	U^{11}	U^{22}	U^{33}	U^{12}	U^{13}	U^{23}
Eu1A	0.01489 (13)	0.00998 (14)	0.01356 (13)	-0.00037 (7)	0.00379 (9)	-0.00035 (8)

O6	0.0446 (16)	0.0207 (15)	0.0244 (14)	0.0096 (12)	0.0121 (12)	0.0042 (12)
O8	0.0355 (15)	0.0197 (15)	0.0206 (15)	0.0018 (11)	0.0114 (13)	-0.0022 (11)
O5	0.0494 (17)	0.0224 (16)	0.0230 (14)	0.0099 (13)	0.0133 (13)	0.0000 (12)
O2	0.0215 (14)	0.0420 (19)	0.0291 (16)	-0.0002 (12)	0.0064 (12)	-0.0073 (13)
O7	0.0425 (16)	0.0182 (15)	0.0244 (14)	0.0085 (12)	0.0060 (12)	0.0020 (12)
O4	0.0320 (16)	0.0368 (18)	0.0329 (17)	0.0101 (12)	0.0045 (13)	-0.0070 (13)
O1	0.0243 (14)	0.048 (2)	0.0420 (17)	0.0037 (13)	0.0095 (13)	-0.0161 (15)
O3	0.0306 (15)	0.0333 (18)	0.0357 (17)	0.0088 (13)	-0.0014 (13)	-0.0089 (14)
C10	0.0242 (19)	0.014 (2)	0.026 (2)	-0.0034 (16)	0.0088 (16)	-0.0023 (17)
C1	0.025 (2)	0.030 (2)	0.029 (2)	-0.0008 (18)	0.0107 (18)	-0.0008 (19)
C9	0.026 (2)	0.021 (2)	0.017 (2)	0.0012 (16)	0.0008 (17)	0.0012 (16)
C8	0.028 (2)	0.027 (2)	0.028 (2)	0.0023 (18)	0.0054 (18)	-0.0028 (19)
C2	0.025 (2)	0.033 (3)	0.035 (2)	0.0063 (17)	0.0074 (19)	-0.0015 (19)
C5	0.030 (2)	0.035 (3)	0.036 (2)	0.0084 (18)	0.005 (2)	-0.004 (2)
C6	0.031 (3)	0.044 (3)	0.056 (3)	0.013 (2)	-0.010 (2)	-0.020 (2)
C3	0.031 (2)	0.048 (3)	0.058 (3)	0.009 (2)	-0.006 (2)	-0.017 (3)
C7	0.035 (2)	0.046 (3)	0.052 (3)	0.015 (2)	0.001 (2)	-0.016 (3)
C4	0.042 (3)	0.053 (3)	0.049 (3)	0.018 (2)	-0.003 (2)	-0.019 (3)
N2	0.033 (4)	0.064 (5)	0.081 (6)	0.026 (3)	-0.007 (4)	-0.040 (4)
N3	0.033 (4)	0.064 (5)	0.081 (6)	0.026 (3)	-0.007 (4)	-0.040 (4)
N1	0.033 (4)	0.064 (5)	0.081 (6)	0.026 (3)	-0.007 (4)	-0.040 (4)
Eu1B	0.0590 (12)	0.0319 (11)	0.0319 (10)	-0.0013 (7)	0.0090 (8)	-0.0028 (7)
O9W	0.076 (3)	0.056 (2)	0.044 (2)	-0.014 (2)	0.0174 (19)	0.0008 (19)

Geometric parameters (\AA , $^\circ$)

Eu1A—Eu1A ⁱ	4.0868 (4)	O4—C8	1.264 (4)
Eu1A—O6	2.521 (2)	O4—Eu1B ^{vii}	2.468 (3)
Eu1A—O8 ⁱⁱ	2.562 (2)	O1—C1	1.266 (4)
Eu1A—O8 ⁱⁱⁱ	2.508 (3)	O3—C8	1.272 (4)
Eu1A—O5	2.508 (2)	O3—Eu1B	2.281 (3)
Eu1A—O2 ⁱ	2.476 (2)	C10—C9	1.558 (5)
Eu1A—O7 ⁱⁱ	2.444 (3)	C1—C2	1.497 (5)
Eu1A—O4 ^{iv}	2.604 (3)	C8—C5	1.484 (5)
Eu1A—O1	2.375 (2)	C2—C3	1.375 (5)
Eu1A—O3 ^{iv}	2.470 (3)	C2—C7	1.393 (6)
O6—C10	1.247 (4)	C5—C6	1.386 (6)
O6—Eu1B ^v	2.445 (3)	C5—C4	1.398 (6)
O8—C10	1.256 (4)	C6—C7	1.386 (6)
O5—C9	1.247 (4)	C3—C4	1.408 (6)
O5—Eu1B ^{iv}	2.811 (3)	C3—N1	1.368 (14)
O2—C1	1.261 (4)	C7—N3	1.343 (13)
O7—C9	1.247 (4)	C4—N2	1.387 (8)
O7—Eu1B ^{vi}	2.349 (3)	Eu1B—O9W	2.317 (4)
O6—Eu1A—Eu1A ⁱ	147.91 (6)	Eu1B ^{vi} —O7—Eu1A ^{ix}	99.74 (10)
O6—Eu1A—O8 ⁱⁱ	129.40 (8)	C8—O4—Eu1A ^x	91.4 (2)
O6—Eu1A—O4 ^{iv}	68.33 (9)	C8—O4—Eu1B ^{vii}	134.7 (3)

O8 ⁱⁱⁱ —Eu1A—Eu1A ⁱ	36.75 (5)	Eu1B ^{vii} —O4—Eu1A ^x	92.50 (9)
O8 ⁱⁱ —Eu1A—Eu1A ⁱ	35.85 (6)	C1—O1—Eu1A	143.2 (2)
O8 ⁱⁱⁱ —Eu1A—O6	137.05 (8)	C8—O3—Eu1A ^x	97.5 (2)
O8 ⁱⁱⁱ —Eu1A—O8 ⁱⁱ	72.60 (9)	C8—O3—Eu1B	153.3 (3)
O8 ⁱⁱ —Eu1A—O4 ^{iv}	111.70 (8)	Eu1B—O3—Eu1A ^x	109.19 (11)
O8 ⁱⁱⁱ —Eu1A—O4 ^{iv}	145.39 (9)	O6—C10—O8	126.6 (3)
O5—Eu1A—Eu1A ⁱ	108.73 (6)	O6—C10—C9	117.1 (3)
O5—Eu1A—O6	64.84 (8)	O8—C10—C9	116.3 (3)
O5—Eu1A—O8 ⁱⁱⁱ	75.76 (8)	O2—C1—O1	123.6 (3)
O5—Eu1A—O8 ⁱⁱ	138.85 (8)	O2—C1—C2	119.8 (4)
O5—Eu1A—O4 ^{iv}	109.32 (8)	O1—C1—C2	116.6 (3)
O2 ⁱ —Eu1A—Eu1A ⁱ	69.48 (6)	O5—C9—C10	117.2 (3)
O2 ⁱ —Eu1A—O6	78.84 (8)	O7—C9—O5	126.9 (4)
O2 ⁱ —Eu1A—O8 ⁱⁱⁱ	73.70 (9)	O7—C9—C10	115.9 (3)
O2 ⁱ —Eu1A—O8 ⁱⁱ	73.49 (8)	O4—C8—Eu1A ^x	63.02 (19)
O2 ⁱ —Eu1A—O5	72.87 (8)	O4—C8—O3	119.9 (3)
O2 ⁱ —Eu1A—O4 ^{iv}	140.91 (9)	O4—C8—C5	121.5 (3)
O7 ⁱⁱ —Eu1A—Eu1A ⁱ	98.87 (6)	O3—C8—Eu1A ^x	56.94 (18)
O7 ⁱⁱ —Eu1A—O6	70.07 (9)	O3—C8—C5	118.6 (4)
O7 ⁱⁱ —Eu1A—O8 ⁱⁱ	64.12 (8)	C5—C8—Eu1A ^x	174.2 (3)
O7 ⁱⁱ —Eu1A—O8 ⁱⁱⁱ	134.20 (8)	C3—C2—C1	120.9 (4)
O7 ⁱⁱ —Eu1A—O5	130.79 (9)	C3—C2—C7	119.9 (4)
O7 ⁱⁱ —Eu1A—O2 ⁱ	80.22 (9)	C7—C2—C1	119.1 (4)
O7 ⁱⁱ —Eu1A—O4 ^{iv}	69.26 (8)	C6—C5—C8	119.1 (4)
O7 ⁱⁱ —Eu1A—O3 ^{iv}	119.41 (9)	C6—C5—C4	118.5 (4)
O4 ^{iv} —Eu1A—Eu1A ⁱ	137.47 (6)	C4—C5—C8	122.4 (4)
O1—Eu1A—Eu1A ⁱ	65.16 (6)	C5—C6—C7	122.5 (4)
O1—Eu1A—O6	146.09 (8)	C2—C3—C4	121.2 (4)
O1—Eu1A—O8 ⁱⁱ	69.59 (9)	N1—C3—C2	125.9 (7)
O1—Eu1A—O8 ⁱⁱⁱ	70.84 (8)	N1—C3—C4	109.9 (7)
O1—Eu1A—O5	122.76 (9)	C6—C7—C2	118.6 (4)
O1—Eu1A—O2 ⁱ	134.63 (9)	N3—C7—C2	127.1 (6)
O1—Eu1A—O7 ⁱⁱ	105.55 (9)	N3—C7—C6	113.1 (6)
O1—Eu1A—O4 ^{iv}	78.60 (9)	C5—C4—C3	119.0 (4)
O1—Eu1A—O3 ^{iv}	75.28 (9)	N2—C4—C5	124.2 (5)
O3 ^{iv} —Eu1A—Eu1A ⁱ	130.96 (7)	N2—C4—C3	116.0 (5)
O3 ^{iv} —Eu1A—O6	78.21 (9)	O6 ^v —Eu1B—O5 ^x	70.24 (9)
O3 ^{iv} —Eu1A—O8 ⁱⁱⁱ	104.11 (8)	O6 ^v —Eu1B—O4 ^{xi}	71.76 (10)
O3 ^{iv} —Eu1A—O8 ⁱⁱ	143.79 (9)	O7 ^{xii} —Eu1B—O6 ^v	72.95 (10)
O3 ^{iv} —Eu1A—O5	69.54 (8)	O7 ^{xii} —Eu1B—O5 ^x	101.31 (10)
O3 ^{iv} —Eu1A—O2 ⁱ	141.55 (9)	O7 ^{xii} —Eu1B—O4 ^{xi}	73.14 (10)
O3 ^{iv} —Eu1A—O4 ^{iv}	51.17 (8)	O4 ^{xi} —Eu1B—O5 ^x	141.46 (10)
C10—O6—Eu1A	120.2 (2)	O3—Eu1B—O6 ^v	99.37 (11)
C10—O6—Eu1B ^v	143.1 (2)	O3—Eu1B—O5 ^x	66.84 (9)
C10—O8—Eu1A ^{viii}	126.6 (2)	O3—Eu1B—O7 ^{xii}	167.83 (13)
C10—O8—Eu1A ^{ix}	118.0 (2)	O3—Eu1B—O4 ^{xi}	114.01 (12)
C9—O5—Eu1A	120.6 (2)	O3—Eu1B—O9W	100.09 (12)
C9—O5—Eu1B ^{iv}	110.2 (2)	O9W—Eu1B—O6 ^v	146.74 (13)

C1—O2—Eu1A ⁱ	130.7 (2)	O9W—Eu1B—O5 ^x	93.23 (12)
C9—O7—Eu1A ^{ix}	123.2 (2)	O9W—Eu1B—O7 ^{xii}	82.84 (12)
C9—O7—Eu1B ^{vi}	137.1 (2)	O9W—Eu1B—O4 ^{xi}	122.82 (13)

Symmetry codes: (i) $-x, -y+1, -z$; (ii) $-x, y-1/2, -z+1/2$; (iii) $x, -y+3/2, z-1/2$; (iv) $-x+1, y+1/2, -z+1/2$; (v) $-x+1, -y+1, -z+1$; (vi) $x-1, -y+3/2, z-1/2$; (vii) $x, -y+1/2, z-1/2$; (viii) $x, -y+3/2, z+1/2$; (ix) $-x, y+1/2, -z+1/2$; (x) $-x+1, y-1/2, -z+1/2$; (xi) $x, -y+1/2, z+1/2$; (xii) $x+1, -y+3/2, z+1/2$.

Hydrogen-bond geometry (Å, °)

<i>D</i> —H... <i>A</i>	<i>D</i> —H	H... <i>A</i>	<i>D</i> ... <i>A</i>	<i>D</i> —H... <i>A</i>
O9W—H9WA...O2 ^{xiii}	1.11 (5)	1.81 (5)	2.904 (4)	171 (5)
O9W—H9WB...O5 ^{xii}	1.10 (5)	1.87 (5)	2.943 (4)	163 (4)
C6—H6...O3	0.93	2.47	2.781 (6)	100
N1—H1B...O2	0.86	2.03	2.736 (16)	139

Symmetry codes: (xii) $x+1, -y+3/2, z+1/2$; (xiii) $-x+1, -y+1, -z$.